Soft-tissue fossilization illuminates the stepwise evolution of the ray-finned fish brain

Rodrigo T. Figueroa[1-2*], Luiz Carlos Weinschütz[3], Sam Giles[4], Matt Friedman[1-2]

1 – Department of Earth and Environmental Sciences, University of Michigan, North University Building, 1100 North University Ave., Ann Arbor, Michigan, 48109, USA
2 – Museum of Paleontology, University of Michigan , Biological Sciences Building, 1105 North University Ave., Ann Arbor, Michigan, 48109, USA
3 – Centro Paleontologico da Universidade do Contestado, CENPALEO, Av. Presidente Nereu Ramos 1071, Jardim Moinho, Mafra, Santa Catarina, 89806-076, Brazil.
4 – School of Geography, Earth and Environmental Sciences, University of Birmingham, Edgbaston, B15 2TT, Birmingham, UK

*rtfiguer@umich.edu; Twitter: @rodrigoichthys

Keywords: Neuroanatomy, Actinopterygii, Paleozoic, telencephalon, Permo-Carboniferous

This PDF file includes:

Main Text
Figures 1 to 4

Temporary reviewer CT data access:
https://www.dropbox.com/scl/fo/6mt3j047t804zbwnjgajl/h?rlkey=70njfjqwle5wqf18dr5aq5vq6&dl=0

Summary

A complex brain is central to the success of backboned animals. However, direct evidence bearing on vertebrate brain evolution comes almost exclusively from extant species, leaving substantial knowledge gaps. Although rare, soft-tissue preservation in fossils can yield unique insights on patterns of neuroanatomical evolution. Paleontological evidence from an exceptionally preserved Pennsylvanian (ca. 318 Ma) actinopterygian, *Coccocephalus*, calls into question prior interpretations of ancestral actinopterygian brain conditions. However, ordering and timing of major evolutionary innovations such as an everted telencephalon, modified meningeal tissues, and hypothalamic inferior lobes remain unclear. Here we report two distinct actinopterygian morphotypes from the latest Carboniferous-earliest Permian (~299 Ma) of Brazil that show extensive soft-tissue preservation of brains, cranial nerves, eyes and potential cardiovascular tissues. These fossils corroborate inferences drawn from *Coccocephalus*, while adding new information about neuroanatomical evolution. Skeletal features indicate that one of these Brazilian morphotypes is more closely related to living actinopterygians than the other, which is also reflected in soft-tissue features. Significantly, the more crownward morphotype shows a key neuroanatomical feature of extant actinopterygians–an everted telencephalon–that is absent in the other morphotype and *Coccocephalus*. All preserved Paleozoic actinopterygian brains show broad similarities including an invaginated cerebellum, hypothalamus inferior lobes, and a small forebrain. In each case, preserved brains are substantially smaller than the enclosing cranial chamber. The neuroanatomical similarities shared by this grade of Permo-Carboniferous actinopterygians reflect probable primitive conditions for actinopterygians, providing a revised model for interpreting brain evolution in a major branch of the vertebrate tree of life.

Introduction

The vertebrate brain is specialized and distinct from that of other animal groups[1]. Jawed vertebrates (gnathostomes) show broad conservation of major brain regions[1,2], but there is wide structural and developmental variation within the group[3] generally ascribed to differences in ecology and behavior. Among living gnathostomes, the roughly 30,000 species of ray-finned (actinopterygian) fishes display many neuroanatomical innovations[1,4] with profound variation in the size of brain regions across lineages[1,5,6]. This diversity of brains mirrors the variety of ray-finned fishes as a whole, reflecting over 350 million years of evolution in a range of aquatic habitats[7,8].

Extant animals provide abundant information about brain structure, but important gaps in our understanding remain. First, the vast majority of living ray-finned fishes belong to Teleostei, which contains roughly 98% of all extant actinopterygian species[7]. Crown teleosts are geologically young, first appearing in the fossil record[9,10] roughly 200 million years after the origin of crown actinopterygians and nearly 300 million years after ray-finned fishes diverged from their lobe-finned sister lineage[9]. Non-teleost actinopterygians provide critical details about neuroanatomical evolution deeper in the ray-finned fish tree, but these depauperate groups often display highly specialized morphologies. Given that early-diverging living ray-finned fishes are highly specialized[7,11,12] there are standing questions on the order and timing of important morphological innovations such as telencephalic eversion, bulging of the cerebellum, and the development of hypothalamus inferior lobes and modified tela choroidea tissues. Second, while actinopterygians have a rich fossil record, few fossils provide evidence for patterns of brain evolution. Cranial endocasts generally represent the only evidence bearing on the neuroanatomy of extinct species, but the constraints they provide are indirect. Furthermore, there is evidence from several vertebrate lineages that endocasts have a varying degree of fit to brain anatomy[13–16] and thus neuroanatomical evidence derived directly from fossil endocasts should be considered with care.

The recent description of a fossil brain in a late Carboniferous ray-finned fish[17], combined with earlier reports of a comparable preservation in a contemporary chondrichthyan[18,19], suggests that fossilized neuroanatomy might be more common than widely assumed. However, the absence of additional extinct comparators limits the impact of these known examples. Here we report new instances of three-dimensional preservation of brains and other soft tissues in ray-finned fishes from the early Permian (Cisuralian, ~298.9-272.9 Ma) Lontras Shale of Brazil, a deposit regarded as a *Konservat-Lagerstätte*[20]. Two distinct actinopterygian morphotypes, differentiated by osteological structure, preserve brains, eyes, and other soft tissues. These specimens challenge interpretations of the evolutionary timing and sequence of innovations in the ray-finned fish brain, illustrating the significance of three-dimensionally preserved soft tissues for comparative studies.

Results

Lontras Shale ray-finned fishes.

The Lontras Shale comprises dark, laminated shales that preserve compressed but essentially complete, articulated specimens[20,21]. Sideritic concretions within these shales contain three-dimensionally preserved skulls[22]. Specimens preserved within concretions show

two distinct taphonomic modes: one where skulls are fully perfused with matrix, and a second where matrix infill within the skull is absent. Micro-computed tomography (μCT) of concretions encompassing both taphonomic modes reveals skeletal anatomy plus soft-tissue structures within and around the braincase and optic capsules. Two different ray-finned fish morphotypes, distinguished on the basis of major osteological traits across the mandibular, hyoid, and branchial arches, as well as the braincase (Figure 1), show soft-tissue preservation. For each of these features, Morphotype I shows a derived state relative to Morphotype II based on comparison with well-preserved Late Devonian taxa that branch from the actinopterygian stem[23]. Osteological data suggests that Morphotype I is closely related to more crownward forms (e.g., the Triassic †*Australosomus*), while CP 584 resembles more stemward taxa from the Devonian and Carboniferous. Taken together with †*Coccocephalus wildi*, these three examples appear to represent a grade on the actinopterygian stem.

Each morphotype is represented by multiple specimens (see START Methods). However, most of our account focuses on two specimens: CP 065 for Morphotype I and CP 584 for Morphotype II (Figure 1, Figure S1). Specimens from this unit show two distinct taphonomic types (complete infill of the cranial cavity by matrix; and dissolution of matrix within the cranial cavity). Although the specimens chosen to represent each morphotype here (CP 065 and CP 584) are preserved in different modes, additional specimens from both morphotypes encompass these two preservation types. Additional specimens (CP 1343, CP 6573) are too incomplete to be assigned to a morphotype but display partial soft-tissue preservation. Precise taxonomic assessment of these two morphotypes is challenging. Previously described taxa from the Lontras Shale are, like many Paleozoic actinopterygians, based on poor type material[21,22] that do not permit us to either assign the morphotypes to existing taxa or alternatively propose new ones. We therefore leave our specimens in open nomenclature pending revision of the Lontras actinopterygian fauna.

Comparative anatomy of fossil morphotypes.

The two fossil morphotypes can be differentiated on the basis of osteological features, some of which indicate that these morphotypes are likely affiliated with different parts of the actinopterygian stem. Morphotype I is distinguished by bearing two ceratohyal ossifications (anterior and posterior), a dorsomesial process on the palatoquadrate for articulation with the braincase without a notch or foramen, large and posterodorsally directed uncinate processes of

the epibranchials, a fossa bridgei that is constrained above the level of the inner ear, and a common midline canal for the olfactory nerves. Morphotype II, on the other hand, shows a single ceratohyal ossification, a semilunar notch on the palatoquadrate marking the basipterygoid articulation, small and dorsally directed uncinate processes of the epibranchials, a wide and well-developed fossa bridgei that extends from the level of the posterodorsal fontanelle to the level of the anterodorsal fontanelle, and paired canals for the olfactory nerves. All the conditions found in Morphotype I are in agreement with a more crownward placement relative to both Morphotype II and *Coccocephalus wildi*, based on information from well-preserved Late Devonian and Triassic taxa[23–25]. Additionally, these two morphotypes differ in several additional traits of more ambiguous polarity including parasphenoid geometry in lateral view (curved dorsally in Morphotype I versus horizontal in Morphotype II), size and shape of the anterodorsal fontanelle (large and oval in Morphotype I, smaller and slit-like in Morphotype II), and proportions of the skeletal labyrinth (external semicircular canal anteroposteriorly long with anterior and posterior limbs at an obtuse angle in Morphotype I compared to Morphotype II)

Fossil brain anatomy.

The brain occupies a small portion of the endocranial cavity in both morphotypes, in agreement with †Coccocephalus[17] and contrary to widespread assumptions[26–28]. It appears more closely associated with the endocranial wall in specimens of Morphotype I due to the preservation of possible meningeal tissues, which appears to be absent in Morphotype II/CP 584, although this could be due to preservation (Figures 2-3). Both morphotypes show clear division of the forebrain, midbrain, and hindbrain, with the midbrain representing the largest division. Cranial nerves from all three regions reaching foramina on the endocranial wall. The gross anatomy of these fossil brains generally corresponds with that of both extant ray-finned fishes[1] and the older stem actinopterygian †*Coccocephalus wildi*[17].

Morphotype I. Small, poorly preserved olfactory bulbs fused into a single median structure lie anteroventral to the telencephalon (ob, Figure 3). The small telencephalon (te, Figure 3) shows indications of eversion, indicated by its V-shaped cross-section (Fig. S9). A pair of asymmetrically diverging structures extends toward the roof of the telencephalic region of the endocast, possibly representing anterior cerebral veins (acv, Figure 3; main choroidal veins of ref.[29]).

The mesencephalon is well-preserved (Figure 3), with the optic tectum represented as a sheet surrounding the mesencephalic ventricles (Figure S6). In dorsal view, the optic tectum forms diverging elliptical lobes. There is no evidence of a protrusion associated with the torus lateralis on the lateroventral wall of the diencephalon and intraventricular projections associated with a torus longitudinalis or torus semicircularis are not apparent (Figure S2, me), although we cannot rule out that these were present, but of limited size. We cannot identify a cerebral aqueduct connecting the mesencephalic ventricles to the more posterior fourth ventricle. A small internal cavity of the brain lies ventral to the fourth ventricle. This might be the extrameningeal space connected to the infundibulum (Figure S6). Small bumps posterior to the mesencephalon that seem to coalesce represent the cerebellum or corpus cerebelli (Figure 3, Figure S2). The posterior part of the hindbrain is a long stalk of circular cross-section, comprising the myelencephalon and spinal cord (sc, Figure 3, Figure S2).

The hypophysis emerges from the ventralmost portion of the diencephalon (hypothalamus) and extends ventrally towards the hypophyseal chamber of the neurocranium. The distal end of the hypophysis bears a small well-differentiated adenohypophysis (adh, Figure 3) that lies dorsal to the parasphenoid. The hypothalamus is elongated with large hypothalamic inferior lobes (hil, Figure 3).

Cranial nerves are partially visible on both sides of the brain. A single thin, poorly preserved olfactory nerve (I) extends into the olfactory canal of the endocavity. The mesencephalon bears an expansion representing the roots of the optic nerves (II; optic chiasma). At the level of the posteriormost portion of the mesencephalic bulbs, the rhombencephalon bears a nucleus that divides into three separate nerves. These appear to be, from anterior to posterior: the main motor branch of the trigeminal nerve (V), a posterior branch of the facial nerve (VII), and the octavolateralis (VIII) complex. Only two branches of the latter complex are well preserved: one interpreted as the anterior branch of the octavolateralis (aVII) nerve; and a second, posteroventrally directed towards the saccular chamber, interpreted as representing the posterior branch of the octavolateralis (pVII). Other branches are too poorly preserved to identify. The vagus nerve (X, Figure 3, Figure S2) extends from the hindbrain and exits the neurocranium through the otico-occipital fissure (Figure 2). It divides into anteriorly- and posteriorly-directed branches, which are here identified as branchial and visceral rami, respectively.

A thin sheet, closely associated with the internal surface of the endocavity, surrounds the brain (mix, Figure 3, Figure S2). It is best developed at the diencephalon-mesencephalon interface and above the rhombencephalon. The membrane connects laterally to the body of the

186 brain, dorsal to most nerve roots, and appears to represent meningeal tissue related to the
187 diencephalic and rhombencephalic tela choroidea.
188
189 *Morphotype II* Brain anatomy for Morphotype II is less clear than for Morphotype I. The poorly
190 preserved telencephalon consists of the left telencephalic bulb (te, Figure 3) and appears to be
191 evaginated, as it is bilobate in cross-section (Figure S1-2). The expanded area of the optic
192 chiasma lies ventral to the telencephalon, immediately posterior to the median optic nerve
193 foramen. The mesencephalon shows similar proportions to Morphotype I (CP 065), but
194 distortion of the mesencephalic ventricles in this specimen suggests taphonomic shrinkage or
195 compression (me, Figure S1-2). Another specimen attributable to Morphotype II (CP 508) shows
196 well-developed mesencephalic ventricles (Figure S2). A possible infundibulum extends more
197 posteriorly than in Morphotype I. The cerebellum bears paired lobes that do not seem to
198 coalesce (Figure 3). Anterodorsal and lateral bands suspend the brain within the endocranial
199 chamber (li_l, li_t, Figure 3), representing possible ligaments (cf. *Polypterus*[30]).
200 The mesencephalon shows clearly defined–but taphonomically compressed–
201 mesencephalic bulbs forming the optic tectum (Figure S1). Thin separation marking the
202 ventricular wall indicates that ventricles were present in life (Figure S1), but they cannot be
203 reconstructed. The optic nerve (II) lies ventral to the mesencephalic bulbs. A small protrusion
204 that could be the origin of the oculomotor nerve (III) is apparent on the right side of the brain
205 near the optic chiasma.
206 A clearly defined crista cerebellaris (cr; Figure 3) extends from the posteriormost portion
207 of the mesencephalic region towards the spinal cord. Small concavities posterior to the
208 mesencephalic bulbs represent the corpus cerebelli, which appears to be invaginated (Figure
209 S6). The rhombencephalic region of the brain shows the expanded nuclei of the trigeminal
210 nerve (V) and hyomandibular trunk of the anteroventral lateral line and facial nerves (AV + VII_{hy};
211 Figure 3). These display an arrangement like Morphotype I, although they are more robust and
212 occupy a more posterior position in Morphotype II. A nodule-like structure, likely formed
213 from taphonomic torsion of the spinal cord, lies posterior to these nuclei. The robust spinal cord
214 extends to reach the foramen magnum. The vagus and accessory spinal nerves are not
215 preserved.
216 A large soft-tissue structure overlies the spinal cord and extends laterally towards the
217 lateral cranial canal (Figure S5). We consider this structure homologous to the myelencephalic
218 gland of chondrosteans and holosteans[17,31].
219

Additional specimens

Other specimens show similar structures to the examples described above, but are less well preserved and do not generally provide additional information on brain anatomy. These include examples of Morphotype I (CP.V 4364, CP.V 7053, CP.V 7227) and Morphotype II (CP 084, CP 577).

Other preserved soft tissues

Apart from the brains, other soft tissues are apparent to varying degrees (Figures 4-5, Figures S3-5. Many specimens preserve eye lenses (Morphotype I: CP 065, CP.V 4364; Morphotype II: CP 084, CP 508), with some showing more extensive preservation of other features. In CP 084, a thin sheet of tissue embraces the mesial half of the eye lens (Figure 5), likely representing the sclera and retina (Figure 4B, 5B). The mesial face of this sheet bears tuberous structure corresponding to the optic nerve. CP 4364 shows scleral tissue dissociated from the displaced eye lens, but attached to the brain via a robust optic nerve tract. Some specimens show possible evidence of extrinsic eye muscles (Figure S3).

Gill filaments are well preserved in several specimens (Morphotype I: CP 065; Morphotype II: CP 084; and indeterminate: CP 1343, CP 6573). The gill filaments are short and robust in both morphotypes, attaching to the lateral margin of the elongate ceratobranchials. Some filaments show the area of attachment to the branchial arch in detail (Figure S4).

Putative cardiovascular elements are poorly preserved in all specimens, with fragments of blood vessels observed in a small number of specimens (Morphotype I: CP 4346, Morphotype II: CP 084, CP 584). However, these do not provide any valuable anatomical information (Figure S5 A-C).

Discussion

Placement and polarity of brain character changes.

Given the osteological variation and polarity of these characters described above, we interpret these two Brazilian morphotypes to form a grade on the actinopterygian stem together with *Coccocephalus* (Figure 6). Thus, these fossils provide insights on the polarity of important neuroanatomical changes along the actinopterygian stem.

Telencephalon eversion versus evagination. In Morphotype I, the telencephalon displays a dorsolateral expansion and ventral compression towards the area of the optic chiasma, resulting in a V-shaped structure in cross-section (Figure S2). This resembles the everted telencephalon geometry of all extant ray-finned fishes. Morphotype II (e.g. CP 584) and †*Coccocephalus*[17], show a contrasting anatomical condition. In cross-section, the telencephalon of these taxa forms a symmetrical bulge with a central cavity but lacking a ventral compression (Figure S1-2). This is similar to the structure in living sarcopterygians and chondrichthyans, and so is interpreted here as representing a plesiomorphic evaginated telencephalon. We therefore place telencephalic eversion as a feature emerging crownward of †*Coccocephalus* but stemward of CP 065 (Figure 6). More information from late Paleozoic fossil brains will be essential for better understanding the timing of origin of the everted condition found in living ray-finned fishes, but current information points to a late Paleozoic origin for the development of this condition.

Hypothalamus inferior lobes. The presence of a hypothalamus inferior lobe in some specimens challenges the current hypothesis of character polarity. Since a hypothalamus inferior lobe is absent in the earliest diverging lineage of crown ray-finned fishes (i.e., cladistians) it was assumed to be a derived feature of actinopterans (crown ray-finned fishes excluding Cladistia[32,33]). However, its presence in some of the Brazilian specimens, as well as in the older †*Coccocephalus*, challenges this hypothesis. Conditions in these probable stem actinopterygians imply the absence of the hypothalamus inferior lobe in cladistians is a reversal within that lineage rather than retention of a primitive arrangement. The apparent absence of a hypothalamus inferior lobe in some of the Brazilian specimens (e.g. CP 584) is likely due to taphonomy and compression of the soft-tissue against the endocranial wall. Future work should investigate the relationship between the actinopterygian hypothalamus inferior lobe and other hypothalamic projections in lobe-finned fishes and chondrichthyans. This is essential to determine if these independently emerged in several lineages or if instead hypothalamic ventral projections are primitive for crown gnathostomes.

Intraventricular projections. Extant actinopterans show well-differentiated intraventricular projections (torus longitudinalis, torus semicircularis) within the second ventricle. These are unique to the group[1]. Cladistians are unique among living ray-finned fishes in lacking a torus longitudinalis and torus semicircularis[1,34]. All known Permo-Carboniferous actinopterygian brains lack evidence for these intraventricular projections, with all examples showing a homogeneous

ventricular margin. Thus, we confirm these intraventricular projections are a derived characteristic of actinopterans.

Meningeal tissues. Aspects of brain suspension within the endocranial cavity are poorly documented among ray-finned fishes. Bjerring[30] described intracranial ligaments supporting the brain of *Polypterus senegalus*, while other extant actinopterygians seem to have a well-developed meningeal tissue that suspends the brain within the neurocranial endocavity (Figueroa, pers. obs.). The Brazilian fossils show both conditions, with Morphotype I bearing a well-developed meningeal tissue above the hindbrain and forebrain while Morphotype II lacks any evidence of meningeal tissue but shows ligament-like structures connecting the brain to the endocranial wall. However, it is possible that the absence of a meningeal tissue in Morphotype II is taphonomic, as the main specimen that our description focuses on (CP 584) is preserved without matrix infill within the braincase. Thus, meningeal tissue could have been lost either during fossilization or during dissolution and loss of the matrix infill or. The meningeal tissue preserved in Morphotype I (CP 065) differs from the brain tissue as it is a very delicate and thin sheet of tissue that attaches to the laterodorsal margins of the brain and expands dorsally following the shape of the endocranial cavity.

Meningeal tissues with associated hematopoietic organs are present in non-teleost ray-finned fishes excluding cladistians. Past work suggested that similar organs would be present in Paleozoic ray-finned fishes based on the presence of an enlarged area octavolateralis and lateral diverticula near the posterior semicircular canal (referred to as the lateral cranial canal) in some fossils[34]. A large mass dorsal to the rhombencephalon of Morphotype II (CP 584) is consistent with a myelencephalic gland (Figure S5). This structure is boomerang-shaped in dorsal view and extends laterally towards the lateral cranial canal. The geometry and position of this structure matches the myelencephalic gland of *Lepisosteus*[35]. Identification of a myelencephalic gland in Morphotype II supports past inferences of its presence in early ray-finned fishes. Its lateral extension is consistent with the well-developed lateral cranial canal found in many Paleozoic ray-finned fishes and early neopterygians[8,34,36]. Pattern suggests the myelencephalic gland of *Lepisosteus* might more closely resemble the plesiomorphic condition, with the tube-shaped gland of chondrosteans and *Amia* being derived. A myelencephalic gland is absent in *Coccocephalus,* CP 065 and *Polypterus*, which all share a robust rhombencephalic tela choroidea modified as a cisterna spinobulbaris, following the interpretation from Jarvik[34]. We cautiously suggest the myelencephalic gland arose deep on the actinopterygian stem, with independent variations

arising within the crown (Figure 6). This agrees with the wide variability of shape and connectivity of the myelencephalic gland in extant taxa[31].

Anterior cerebral vein. The anterior cerebral vein emerges at the level of the posterior end of the orbit and arches dorsomesially above the telencephalon[29,37]. In ray-finned fishes, this vein tends to be well-developed during embryonic and larval stages but is sometimes absent in adults[37]. Allis[38] notes that although the anterior cerebral vein is not noticeable in adult specimens of *Amia*, the paired foramina through which it would pass remain present posterodorsal on the optic capsule wall. In Paleozoic ray-finned fishes (e.g., †*Mimipiscis*, †*Mesopoma*) the canal for the anterior cerebral vein is unpaired and asymmetrical above the telencephalic region of the endocranial cavity[26,39,40]. In some Devonian sarcopterygians (e.g., †*Eusthenopteron*) paired canals are present, but these lay more anterior at the proximal end of the olfactory tracts[34], while in others (e.g., †*Gogonasus andrewsae)* there is a single median canal[41]. Morphotype I (acv, Figure 2) and †*Coccocephalus* show paired but asymmetrical anterior cerebral veins that connect to the velum transversum and the orbital sinus before exiting the brain towards the left side of the skull. The asymmetry and position of these veins is consistent with the canal described in Paleozoic ray-finned fishes. However, the presence of two veins in the fossil specimens indicates that the single canal present in Paleozoic forms held two branches of this vein, which in turn agrees with the presence of paired anterior cerebral veins in living ray-finned fishes.

Future directions in paleoneurology.

The field of paleoneurology has advanced since its early days[42–44] through the study of endocasts as proxy for brain anatomy in several vertebrate groups[26,27,45] and two-dimensional imprints of nerve tissue in some invertebrates[46,47]. However, endocast data remains limited in providing an external model of the brain at best[2] and only loose constraints on morphology in taxa where the volume of the brain is small in comparison to that of the endocavity[48,49]. Three-dimensional preservation of neural soft-tissue structures discovered in fossil fishes by past studies[18] and expanded upon here suggests further tomographic surveys of vertebrates are likely to yield additional examples. Geological context for each of these cases is broadly similar, with fossil skulls preserved in three-dimensions within concretions. Several Paleozoic and early

Mesozoic sites yield three-dimensional heads of actinopterygians within concretions[25,28,50–52], and we are optimistic that further tomographic surveys of this material will yield additional instances of soft tissue preservation. As investigation of other fossils expands the dataset of fossil brains, it might be possible to discern which taphonomic or environmental aspects tend to covary with the preservation of neuroanatomy. This, in turn, can be used to identify material that is most likely to yield soft-tissue structures. Even modest amounts of information on ancient brain anatomy in other branches of the actinopterygian phylogeny–including deeper parts of the actinopterygian stem, the actinopteran stem, and the teleost stem–could provide important new evidence on patterns of neuroanatomical evolution in ray-finned fishes. Examples from other fish lineages have also shown potential for extensive soft-tissue preservation and variation in mode of preservation depending on the type of tissue and position within the body[18,53,54]. Our results suggest that information from fossil soft tissues can have an impact on our understanding of the evolution of deeply branching lineages,helping to identify patterns of morphological change that would be otherwise impossible to interpret only from extant taxa.

The fossils described herein challenge current interpretations of the origin and timing of important morphological innovations, especially within the forebrain. This highlights biases that might arise from reconstructing the phylogenetic history of important morphological innovations based solely on extant species. We expect that with the inclusion of more information on soft tissue anatomy of early vertebrates—gathered from exceptional soft-tissue preservation—we will be able to better understand not only the placement of fossil taxa in relation to the crown, but also revise soft-tissue features of living lineages and determine how far back in geologic time many of these putative synapomorphies of extant clades emerged.

Acknowledgments

We thank the Centro Paleontologico da Universidade do Contestado (CENPALEO) for access and loan of fossil specimens for this project. We thank the Agência Nacional de Mineração (ANM) for processing of international loan permits. We thank R Singer and H Lopez-Fernandez for access to UMMZ collections. RT Figueroa was supported by the Department of Earth and Environmental Sciences at the University of Michigan, the Rackham Graduate Predoctoral Fellowship of the University of Michigan and a Society of Systematics Biologist Graduate Student Research Award. S Giles was supported by a Royal Society Dorothy Hodgkin Research Fellowship (DH1600098). This study was partially supported by NSF EAR 2219007 (M Friedman). This study includes data produced at the CTEES facility at the University of

Michigan, supported by the Department of Earth and Environmental Sciences and College of Literature, Science and the Arts.

Author Contributions: RT Figueroa designed the project, analyzed data, wrote the manuscript and designed figures; LC Weinschutz helped with specimen selection, processing and access; S Giles and M Friedman designed the project and wrote the manuscript.

Declaration of Interests: The authors declare no competing interests.

Figure legends.

Figure 1. Comparison of two morphotypes of actinopterygian fishes from the Lontras Shale, Brazil. Morphotypes differentiated on the basis of osteological traits, showing neurocranium (top), endocast (middle) and hyobranchial apparatus (bottom). c.l, olfactory tract, chy, ceratohyal, fbr, fossa bridgei, hsc, horizontal semicircular canal, psp, parasphenoid, un.p, uncinate processes. Panels not to scale. See also Figures S1-S6.

Figure 2. Brain and neurocranial morphology in Permian actinopterygian fishes. Neurocranium partially removed to show position of brain within the endocavity. Morphotype I (CP 065) and Morphotype II (CP 584) in dorsal (top) and left lateral (bottom) views. Light beige = braincase, dark beige = sliced braincase plane, red = brain, orange = meningeal tissue. a.amp, anterior ampulla, a.ce, auricula cerebelli, adf, anterodorsal fontanelle, c.l, olfactory tract, fm, foramen magnum, hsc, horizontal semicircular canal, me.c, mesencephalic chamber, occ.f, occipital fissure, oct, area octavolateralis, oto, otolith, p.amp, posterior ampulla, pdf, posterodorsal fontanelle, pmy, posterior myodome, psc, posterior semicircular canal, te.c, telencephalic chamber, vc, vestibular chamber. Scale bar = 5 mm for both morphotypes. See also Figures S1, S2, S5, S6.

Figure 3. Brain morphology in Permian actinopterygian fishes. Morphotype I (CP 065) and Morphotype II (CP 584) in dorsal (top) and left-lateral (bottom) view. Line drawings are interpretative schemes based on renders. Red = brain, orange = meningeal tissue. 4v, fourth ventricle, acv, anterior cerebral vein, adh, adenohypophysis, ce, cerebellum, cr, crista cerebellaris, hil, hypothamus inferor lobe, hyp, hypophysis, lil, longitudinal ligament, lit, transverse ligament, me, mesencephalon, mix, meninx, ob, olfactory bulb, occ, occipital nerves, opt, optic chiasma, sc, spinal cord, te, telencephalon, I, olfactory nerve, III, oculomotor nerve, V,

trigeminal nerve, Vmd, mandibular branch of trigeminal, Vmx, maxillary branch of trigeminal, VII, facial nerve, aVII, anterior branch of facial nerve, aVIII, anterior branch of octavolateralis nerve, pVII, posterior branch of octavolateralis nerve, IX, glossopharyngeal nerve, X, vagus nerve, Xbr, branchial branch of vagus nerve, Xv, visceral branch of vagus nerve. Scale bar = 5 mm for both morphotypes. See also Figures S1, S2, S5, S6

Figure 4. *In situ* three-dimensional soft tissues preserved of specimens of Morphotype II. (A) Render of CP 507 showing the brain (red) and eye lenses (gray). (B) Render of the cranium of CP 084 in right-lateral view showing eye soft-tissue. Scale bar = 10 mm. See also Figures S1-S6.

Figure 5. Eye morphology in fossil and extant actinopterygians. (A-C) Morphotype II (CP 084), (D-F) *Polypterus senegalus* (UMMZ 195008). (A,D) µCT sagittal section through eye, (B,E) render of right eye in lateral view, (C-F) render of right eye in mesial view. arm, anterior rectus muscle, dom, dorsal obliquus muscle, drm, dorsal rectus muscle, len, lens, prm, posterior rectus muscle, ret, retina, scl, sclera, vom, ventral obliquus muscle, vrm, ventral rectus muscle, II, optic nerve. Scale bar = 10 mm. See also Figure S3.

Figure 6. Schematic representation of ray-finned fish brain evolution. a, corpus cerebelli (0 = evaginated; 1 = invaginated; illustrated by sagittal sections through idealized hindbrain), b, modified rhombencephalic meningeal tissue (0 = myelencephalic gland; 1 = cisterna spinobulbaris; illustrated by sagittal sections through idealized hindbrain and spinal cord), c, telencephalon (0 = evaginated, 1 = everted; illustrated by axial sections through idealized telencephalon), d, hypothalamus inferior lobes (0 = present; 1 = absent; illustrated by axial sections through idealized diencephalon). Taxon silhouettes obtained from PhyloPic (https://www.phylopic.org/). Extant taxa brain diagrams based on Nieuwenhuys et al[1].

STAR Methods

Resource availability

Lead contact. Information inquiries and resource requests should be sent to the lead author Rodrigo T. Figueroa (rtfiguer@umich.edu)

Material availability. Specimens come from the Lontras Shale strata, within the uppermost Campo Mourão Formation of the Paraná Basin, Brazil. Specimens were collected at the

'campáleo' outcrop in the south of the city of Mafra, state of Santa Catarina, and are deposited in the paleontological collection of the Centro Paleontológico da Universidade do Contestado (CENPALEO-UnC).

Data and code availability. Field and collection data are available at the Centro Paleontologico da Universidade do Contestado, Mafra, Santa Catarina, Brazil. Analyzed specimen data is available on Zenodo at 10.5281/zenodo.10552528.

Experimental model and subject details

Geological setting. Specimens derive from the Lontras Shale sub-section of the Campo Mourão Formation in the Paraná Basin, Brazil. The age of the Lontras Shale unit is estimated between the latest Carboniferous and earliest Permian based on both radiometric dating and biostratigraphy[47–51]. The Lontras Shale is a stratigraphic marker within the Paraná Basin that is related to a maximum marine flooding event[52]. The lithology, stratigraphy and paleobiota of the Lontras Shale suggest deposition in a restricted marine setting, such as a fjord[53]. Specimens analyzed here are preserved in three dimensions and within sideritic concretions[22]. Preservation of specimens varies as in a few examples (e.g. CP 065, CP 508, CP.V 4364) sediment is found within the fossilized skulls, while in others (e.g. CP 577, CP 584) sediment within the fossil seems to have been lost during diagenetic and post-diagenetic processes. In one specimen (CP.V 7053) the sediment within the skull seems to have been recrystallized.

Fossil material. All fossil specimens analyzed in this work (CP 065, CP.V 4364, CP.V 7053, CP.V 7227, CP 084, CP 508, CP 577, CP 584) were collected in the late Carboniferous to Early Permian Campo Mourão Formation in the surroundings of the city of Mafra, Santa Catarina, Brazil. *Morphotype I*: CP 065, CP.V 4364, CP.V 7053, CP.V 7227; *Morphotype II*: CP 084, CP 508, CP 577, CP 584

Extant species material. This study contains data acquired from ethanol preserved specimens from the University of Michigan Museum of Zoology collection. Figured specimens of *Polypterus senegalus* (UMMZ 195008), *Amia calva* (UMMZ 160805, UMMZ, 235291) and *Lepisosteus ocelatus* (UMMZ 196974).

Methods details

Specimen Visualization. The fossil specimens were scanned with the Nikon XT H 225 ST scanner of the CTEES facility in the Department of Earth and Environmental Sciences, University of Michigan. Detailed scan parameters can be found in Table S1. Segmentation of

the resulting data was completed in Mimics 25.0 (Materialise, Leuven, Belgium) and further imaging of the obtained .ply 3D models was done in Blender 4.0[54]. Comparative extant species Iodine enhanced µCT data was collected following the guidelines described in Kolmann et al.[55]

Quantification and statistical analysis. No statistical analyses were performed for this work.

References

1. Nieuwenhuys, R., ten Donkelaar, H.J., and Nicholson, C. (1998). The Central Nervous System of Vertebrates (Springer Berlin Heidelberg) 10.1007/978-3-642-18262-4.
2. Northcutt, R.G. (2002). Understanding Vertebrate Brain Evolution. Integrative and Comparative Biology *42*, 743–756.
3. Striedter, G.F., and Northcutt, R.G. (2019). Synthesis: Patterns and Principles. In Brains Through Time: A Natural History of Vertebrates, G. F. Striedter and R. G. Northcutt, eds. (Oxford University Press), p. 0. 10.1093/oso/9780195125689.003.0007.
4. Nieuwenhuys, R. (1982). An overview of the organization of the brain of actinopterygian fishes. Integrative and Comparative Biology *22*, 287–310. 10.1093/icb/22.2.287.
5. Northcutt, R.G., and Wullimann, M.F. (1988). The Visual System in Teleost Fishes: Morphological Patterns and Trends. In Sensory Biology of Aquatic Animals, J. Atema, R. R. Fay, A. N. Popper, and W. N. Tavolga, eds. (Springer), pp. 515–552.
6. Northcutt, R.G. (2008). Forebrain evolution in bony fishes. Brain Research Bulletin *75*, 191–205. 10.1016/j.brainresbull.2007.10.058.
7. Nelson, J.S., Grande, T.C., and Wilson, M.V.H. (2016). Fishes of the World (John Wiley & Sons).
8. Friedman, M., and Giles, S. (2016). Actinopterygians: the ray-finned fishes—an explosion of diversity. In Evolution of the vertebrate ear : evidence from the fossil record, J. A. Clack, R. R. Fay, and A. N. Popper, eds. (Springer International Publishing), pp. 17–49. 10.1007/978-3-319-46661-3_2.
9. Friedman, M. (2022). The Macroevolutionary History of Bony Fishes: A Paleontological View. Annual Review of Ecology, Evolution, and Systematics *53*, 353–377. 10.1146/annurev-ecolsys-111720-010447.
10. Arratia, G., and Schultze, H.-P. (2024). The oldest teleosts (Teleosteomorpha): their early taxonomic, phenotypic, and ecological diversification during the Triassic. Fossil Record *27*, 29–53. 10.3897/fr.27.115970.
11. Allis, E.P. (1922). The Cranial Anatomy of *Polypterus*, with Special Reference to *Polypterus bichir*. Journal of anatomy *56*, 189-294.43.
12. Friedman, M. (2015). The early evolution of ray-finned fishes. Palaeontology *58*, 213–228. 10.1111/pala.12150.
13. Dutel, H., Galland, M., Tafforeau, P., Long, J.A., Fagan, M.J., Janvier, P., Herrel, A., Santin, M.D., Clément, G., and Herbin, M. (2019). Neurocranial development of the coelacanth and the evolution of the sarcopterygian head. Nature *569*, 556–559. 10.1038/s41586-019-1117-3.
14. Fabbri, M., Mongiardino Koch, N., Pritchard, A.C., Hanson, M., Hoffman, E., Bever, G.S., Balanoff, A.M., Morris, Z.S., Field, D.J., Camacho, J., et al. (2017). The skull roof tracks the brain during the evolution and development of reptiles including birds. Nat Ecol Evol *1*, 1543–1550. 10.1038/s41559-017-0288-2.
15. Clement, A.M., Nysjö, J., Strand, R., and Ahlberg, P.E. (2015). Brain - Endocast relationship in the Australian lungfish, *Neoceratodus forsteri*, elucidated from tomographic data (Sarcopterygii: Dipnoi). PLoS ONE *10*. 10.1371/journal.pone.0141277.

16. Clement, A.M., Mensforth, C.L., Challands, T.J., Collin, S.P., and Long, J.A. (2021). Brain Reconstruction Across the Fish-Tetrapod Transition; Insights From Modern Amphibians. Frontiers in Ecology and Evolution *9*. 10.3389/fevo.2021.640345.
17. Figueroa, R.T., Goodvin, D., Kolmann, M.A., Coates, M.I., Caron, A.M., Friedman, M., and Giles, S. (2023). Exceptional fossil preservation and evolution of the ray-finned fish brain. Nature *614*, 486–491. 10.1038/s41586-022-05666-1.
18. Pradel, A., Langer, M., Maisey, J.G., Geffard-Kuriyama, D., Cloetens, P., Janvier, P., and Tafforeau, P. (2009). Skull and brain of a 300-million-year-old chimaeroid fish revealed by synchrotron holotomography. Proceedings of the National Academy of Sciences of the United States of America *106*, 5224–5228. 10.1073/pnas.0807047106.
19. Pradel, A. (2010). Skull and brain anatomy of Late Carboniferous Sibyrhynchidae (Chondrichthyes, Iniopterygia) from Kansas and Oklahoma (USA). Geodiversitas *32*, 595–661. 10.5252/g2010n4a2.
20. Saldanha, J.P., Del Mouro, L., Horodyski, R.S., Ritter, M. do N., and Schmidt-Neto, H. (2022). Taphonomy and Paleoecology of Lontras Shale Lagerstätte: Detailing the Interglacial Apex of a Late Paleozoic Ice Age Temperate Fjord. Preprint, 10.2139/ssrn.4151382 10.2139/ssrn.4151382.
21. Malabarba, M.C.L. (1988). A new genus and species of stem group actinopteran fish from the Lower Permian of Santa Catarina State, Brazil. Zoological Journal of the Linnean Society *94*, 287–299.
22. Hamel, M. (2005). A new lower actinopterygian from the Early Permian of the Paraná Basin , Brazil. Journal of Vertebrate Paleontology *25*, 19–26.
23. Giles, S., Darras, L., Clément, G., Blieck, A., and Friedman, M. (2015). An exceptionally preserved Late Devonian actinopterygian provides a new model for primitive cranial anatomy in ray-finned fishes. Proceedings of the Royal Society B: Biological Sciences *282*. 10.1098/rspb.2015.1485.
24. Giles, S., Feilich, K., Warnock, R.C.M., Pierce, S.E., and Friedman, M. (2023). A Late Devonian actinopterygian suggests high lineage survivorship across the end-Devonian mass extinction. Nat Ecol Evol *7*, 10–19. 10.1038/s41559-022-01919-4.
25. Nielsen, E. (1949). Studies on Triassic fishes from East Greenland II. *Australosomus* and *Birgeria* (C.A. Reitzels Forlag).
26. Coates, M.I. (1999). Endocranial preservation of a Carboniferous actinopterygian from Lancashire, UK, and the interrelationships of primitive actinopterygians. Philosophical Transactions of the Royal Society B: Biological Sciences *354*, 435–462. 10.1098/rstb.1999.0396.
27. Giles, S., and Friedman, M. (2014). Virtual reconstruction of endocast anatomy in early ray-finned fishes (Osteichthyes, Actinopterygii). Journal of Paleontology *88*, 636–651. 10.1666/13-094.
28. Moodie, R.L. (1915). A new fish brain from the coal measures of Kansas, with a review of other fossil brains. Journal of Comparative Neurology *25*, 135–181. 10.1002/cne.900250203.
29. Weiger, T., Lametschwandtner, A., Kotrschal, K., and Krautgartner, W. -D (1988). Vascularization of the telencephalic choroid plexus of a ganoid fish [Acipenser ruthenus (L.)]. American Journal of Anatomy *182*, 33–41. 10.1002/AJA.1001820104.
30. Bjerring, H.C. (1991). Two Intracranial Ligaments Supporting the Brain of the Brachiopterygian Fish Polypterus senegalus. Acta Zoologica *72*, 41–47. 10.1111/j.1463-6395.1991.tb00314.x.
31. van der Horst, C.J. (1925). The myelencephalic gland of *Polyodon*, *Acipenser* and *Amia*. Koninklijke Akademie van Wetenschappen te Amsterdam Proceedings of the Section of Sciences *28*, 432–442.
32. Rustamov, E.K. (2006). Organization of hypothalamic area of diencephalon in the sturgeons. J Evol Biochem Phys *42*, 342–353. 10.1134/S0022093006030148.

581 33. Schmidt, M. (2020). Evolution of the hypothalamus and inferior lobe in ray-finned fishes. Brain,
582 Behavior and Evolution *95*, 302–316. 10.1159/000505898.
583 34. Jarvik, E. (1980). Basic structure and evolution of vertebrates (Academic Press).
584 35. Chandler, A.C. (1911). On a lymphoid structure lying over the myelencephalon of *Lepisosteus*.
585 University of California Publications in Zoology *9*, 85–104. 10.5962/bhl.title.26215.
586 36. Giles, S., Rogers, M., and Friedman, M. (2018). Bony labyrinth morphology in early
587 neopterygian fishes (Actinopterygii: Neopterygii). J Morphol *279*, 426–440. 10.1002/jmor.20551.
588 37. Bertmar, G. (1965). On the Development of the Jugular and Cerebral Veins in Fishes.
589 Proceedings of the Zoological Society of London *144*, 87–129. 10.1111/j.1469-
590 7998.1965.tb05168.x.
591 38. Allis, E.P. (1897). The cranial muscle and cranial and first spinal nerves in *Amia calva*. Journal
592 of Morphology *XII*, 487–809.
593 39. Hamel, M.-H., and Poplin, C. (2008). The braincase anatomy of *Lawrenciella schaefferi* ,
594 actinopterygian from the Upper Carboniferous of Kansas (USA). Journal of Vertebrate
595 Paleontology *28*, 989–1006. 10.1671/0272-4634-28.4.989.
596 40. Gardiner, B.G. (1984). The relationship of the palaeoniscid fishes, a review based on new
597 specimens of *Mimia* and *Moythomasia* from the Upper Devonian of Western Australia. Bull. Br.
598 nat. Hist. *37*, 173–428.
599 41. Holland, T. (2014). The endocranial anatomy of *Gogonasus andrewsae* Long, 1985 revealed
600 through micro CT-scanning. Earth and Environmental Science Transactions of the Royal
601 Society of Edinburgh *105*, 9–34. 10.1017/S1755691014000164.
602 42. Stensiö, E. (1963). The brain and the cranial nerves in fossil, lower craniate vertebrates.
603 Skriflter Ulgitt Av Det Norske Videnskaps-Akademi, 1–120.
604 43. Buchholtz, E.A., and Seyfarth, E.-A. (1999). The gospel of the fossil brain: Tilly Edinger and the
605 science of paleoneurology. Brain Research Bulletin *48*, 351–361. 10.1016/S0361-
606 9230(98)00174-9.
607 44. Edinger, T. (1964). Recent Advances in Paleoneurology. Progress in Brain Research *6*, 147–
608 160.
609 45. Zhu, Y., Giles, S., Young, G.C., Hu, Y., Bazzi, M., Ahlberg, P.E., Zhu, M., and Lu, J. (2021).
610 Endocast and Bony Labyrinth of a Devonian “Placoderm” Challenges Stem Gnathostome
611 Phylogeny. Current Biology *31*, 1112-1118.e4. 10.1016/j.cub.2020.12.046.
612 46. Ma, X., Hou, X., Edgecombe, G.D., and Strausfeld, N.J. (2012). Complex brain and optic lobes
613 in an early Cambrian arthropod. Nature *490*, 258–261. 10.1038/nature11495.
614 47. Cong, P., Ma, X., Hou, X., Edgecombe, G.D., and Strausfeld, N.J. (2014). Brain structure
615 resolves the segmental affinity of anomalocaridid appendages. Nature *513*, 538–542.
616 10.1038/nature13486.
617 48. Watanabe, A., Gignac, P.M., Balanoff, A.M., Green, T.L., Kley, N.J., and Norell, M.A. (2019).
618 Are endocasts good proxies for brain size and shape in archosaurs throughout ontogeny?
619 Journal of Anatomy *234*, 291–305. 10.1111/joa.12918.
620 49. Challands, T.J., Pardo, J.D., and Clement, A.M. (2020). Mandibular musculature constrains
621 brain–endocast disparity between sarcopterygians. Royal Society Open Science *7*, 200933.
622 10.1098/rsos.200933.
623 50. Schaeffer, B., and Dalquest, W.W. (1978). A Palaeonisciform Braincase from the Permian of
624 Texas, With Comments on Cranial Fissures and the Posterior Myodome. American Museum
625 Novitates *2658*, 1–15.
626 51. Woodward, A.S. (1910). On some Permo-Carboniferous fishes from Madagascar. Annals and
627 Magazine of Natural History *5*, 1–6. 10.1080/00222931008692719.
628 52. Pradel, A., Maisey, J.G., Mapes, R.H., and Kruta, I. (2016). First evidence of an intercalar bone
629 in the braincase of “palaeonisciform” actinopterygians, with a virtual reconstruction of a new
630 braincase of *Lawrenciella* Poplin, 1984 from the Carboniferous of Oklahoma. Geodiversitas *38*,
631 489–504. 10.5252/g2016n4a2.

632 53. Trinajstic, K., Marshall, C., Long, J., and Bifield, K. (2007). Exceptional preservation of nerve
633 and muscle tissues in Late Devonian placoderm fish and their evolutionary implications. Biology
634 Letters *3*, 197–200. 10.1098/rsbl.2006.0604.
635 54. Trinajstic, K., Long, J.A., Sanchez, S., Boisvert, C.A., Snitting, D., Tafforeau, P., Dupret, V.,
636 Clement, A.M., Currie, P.D., Roelofs, B., et al. (2022). Exceptional preservation of organs in
637 Devonian placoderms from the Gogo Lagerstätte. Science *377*, 1311–1314.
638 10.1126/science.abf3289.
639 55. Cagliari, J., Philipp, R.P., Buso, V.V., Netto, R.G., Klaus Hillebrand, P., da Cunha Lopes, R.,
640 Stipp Basei, M.A., and Faccini, U.F. (2016). Age constraints of the glaciation in the Paraná
641 Basin: evidence from new U–Pb dates. Journal of the Geological Society *173*, 871–874.
642 10.1144/jgs2015-161.
643 56. Valdez Buso, V., Aquino, C.D., Paim, P.S.G., de Souza, P.A., Mori, A.L., Fallgatter, C., Milana,
644 J.P., and Kneller, B. (2019). Late Palaeozoic glacial cycles and subcycles in western
645 Gondwana: Correlation of surface and subsurface data of the Paraná Basin, Brazil.
646 Palaeogeography, Palaeoclimatology, Palaeoecology *531*, 108435.
647 10.1016/j.palaeo.2017.09.004.
648 57. Griffis, N.P., Montañez, I.P., Mundil, R., Richey, J., Isbell, J., Fedorchuk, N., Linol, B., Iannuzzi,
649 R., Vesely, F., Mottin, T., et al. (2019). Coupled stratigraphic and U-Pb zircon age constraints on
650 the late Paleozoic icehouse-to-greenhouse turnover in south-central Gondwana. Geology *47*,
651 1146–1150. 10.1130/G46740.1.
652 58. Holz, M., França, A.B., Souza, P.A., Iannuzzi, R., and Rohn, R. (2010). A stratigraphic chart of
653 the Late Carboniferous/Permian succession of the eastern border of the Paraná Basin, Brazil,
654 South America. Journal of South American Earth Sciences *29*, 381–399.
655 10.1016/j.jsames.2009.04.004.
656 59. Wilner, E., Lemos, V.B., and Scomazzon, A.K. (2016). Associações naturais de conodontes
657 Mesogondolella spp., Grupo Itararé, Cisuraliano da Bacia do Paraná. Gaea - Journal of
658 Geoscience *9*, 30–36. 10.4013/gaea.2016.91.02.
659 60. França, A.B., and Potter, P.E. (1991). Stratigraphy and Reservoir Potential of Glacial Deposits
660 on the Itararé Group (Carboniferous-Permian), Paraná Basin, Brazil. The American Association
661 of Petroleum Geologists Bulletin *75*, 62–85.
662 61. Mouro, L.D., Rakociński, M., Marynowski, L., Pisarzowska, A., Musabelliu, S., Zatoń, M.,
663 Carvalho, M.A., Fernandes, A.C.S., and Waichel, B.L. (2017). Benthic anoxia, intermittent photic
664 zone euxinia and elevated productivity during deposition of the Lower Permian, post-glacial
665 fossiliferous black shales of the Paraná Basin, Brazil. Global and Planetary Change *158*, 155–
666 172. 10.1016/j.gloplacha.2017.09.017.
667 62. Garwood, R., and Dunlop, J. (2014). The walking dead: Blender as a tool for paleontologists
668 with a case study on extinct arachnids. Journal of Paleontology *88*, 735–746. 10.1666/13-088.
669 63. Kolmann, M.A., Nagesan, R.S., Andrews, J.V., Borstein, S.R., Figueroa, R.T., Singer, R.A.,
670 Friedman, M., and López-Fernández, H. (2023). DiceCT for fishes: recommendations for pairing
671 iodine contrast agents with μCT to visualize soft tissues in fishes. Journal of Fish Biology *n/a*.
672 10.1111/jfb.15320.

REAGENT or RESOURCE	SOURCE	IDENTIFIER
Biological samples		
Polypterus senegalus	University of Michigan Museum of Zoology	UMMZ 195008
Amia calva (juvenile)	University of Michigan Museum of Zoology	UMMZ 160805
Amia calva (adult)	University of Michigan Museum of Zoology	UMMZ 235291
Lepisosteus ocelatus	University of Michigan Museum of Zoology	UMMZ 196974
Chemicals, peptides, and recombinant proteins		
Ethanol 140 proof	Decon Laboratories Inc.	CAS #64-17-5
Potassium Iodine	Spectrum Chemical MFG Corp.	CAS #7681-11-0
Iodine, Crystalline, 99.5%	thermo scientific	CAS #7553-56-2
Deposited data		
Polypterus senegalus	University of Michigan Museum of Zoology	UMMZ 195008
Amia calva (juvenile)	University of Michigan Museum of Zoology	UMMZ 160805
Amia calva (adult)	University of Michigan Museum of Zoology	UMMZ 235291
Lepisosteus ocelatus	University of Michigan Museum of Zoology	UMMZ 196974
Concretionary fossil specimens	Centro Paleontologico da Universidade do Contestado, CENPALEO	CP 065, CP.V 4364, CP.V 7053, CP.V 7227, CP 084, CP 508, CP 577, CP 584
Specimen and CT data	Zenodo	10.5281/zenodo.10552528
Software and algorithms		
Blender 3D modeling software	https://www.blender.org/	Blender 4.0
Materialise Mimics	https://www.materialise.com/en/healthcare/mimics-innovation-suite/mimics	Mimics 25.0

Highlights

- Soft-tissue preservation is found in late Paleozoic ray-finned fishes from Brazil
- Brain anatomy differs among fossil taxa
- One of these fossils represents the oldest evidence of an everted telencephalon
- The fossil taxa bear a mosaic of 'primitive' and 'derived' characters

eTOC blurb:

Figueroa *et al*. show that soft-tissue preservation in fossil ray-finned fishes is informative for interpreting evolution of neuroanatomy. Using X-ray micro-tomography, they find key differences in brain morphology among extinct taxa. These fossils indicate a more complex evolutionary history for ray-finned fish brains than previously anticipated.

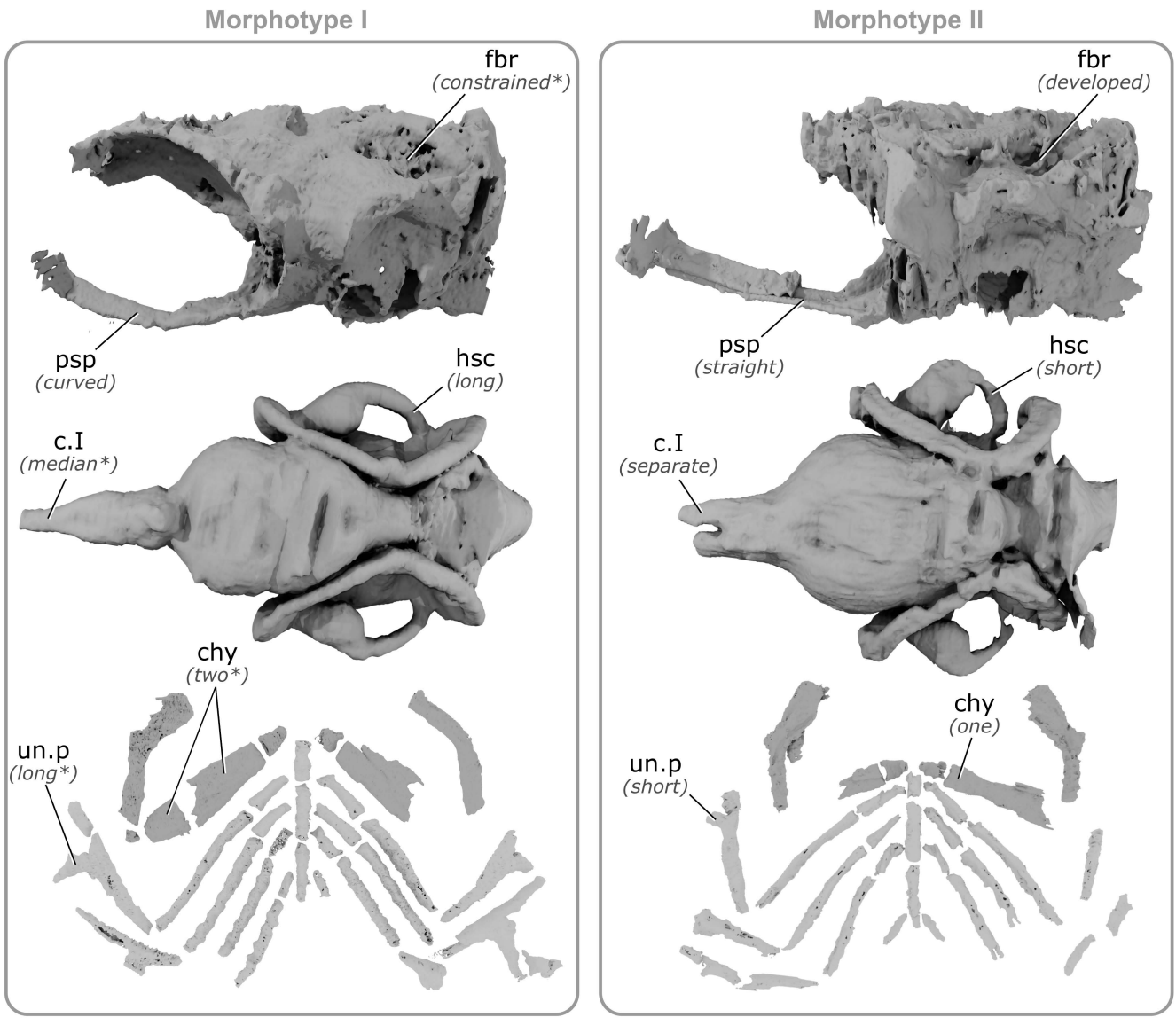
Morphotype I
fbr
(constrained*)
psp
(curved)
hsc
(long)
c.I
(median*)
chy
(two*)
un.p
(long*)
Morphotype II
fbr
(developed)
psp
(straight)
hsc
(short)
c.I
(separate)
chy
(one)
un.p
(short)

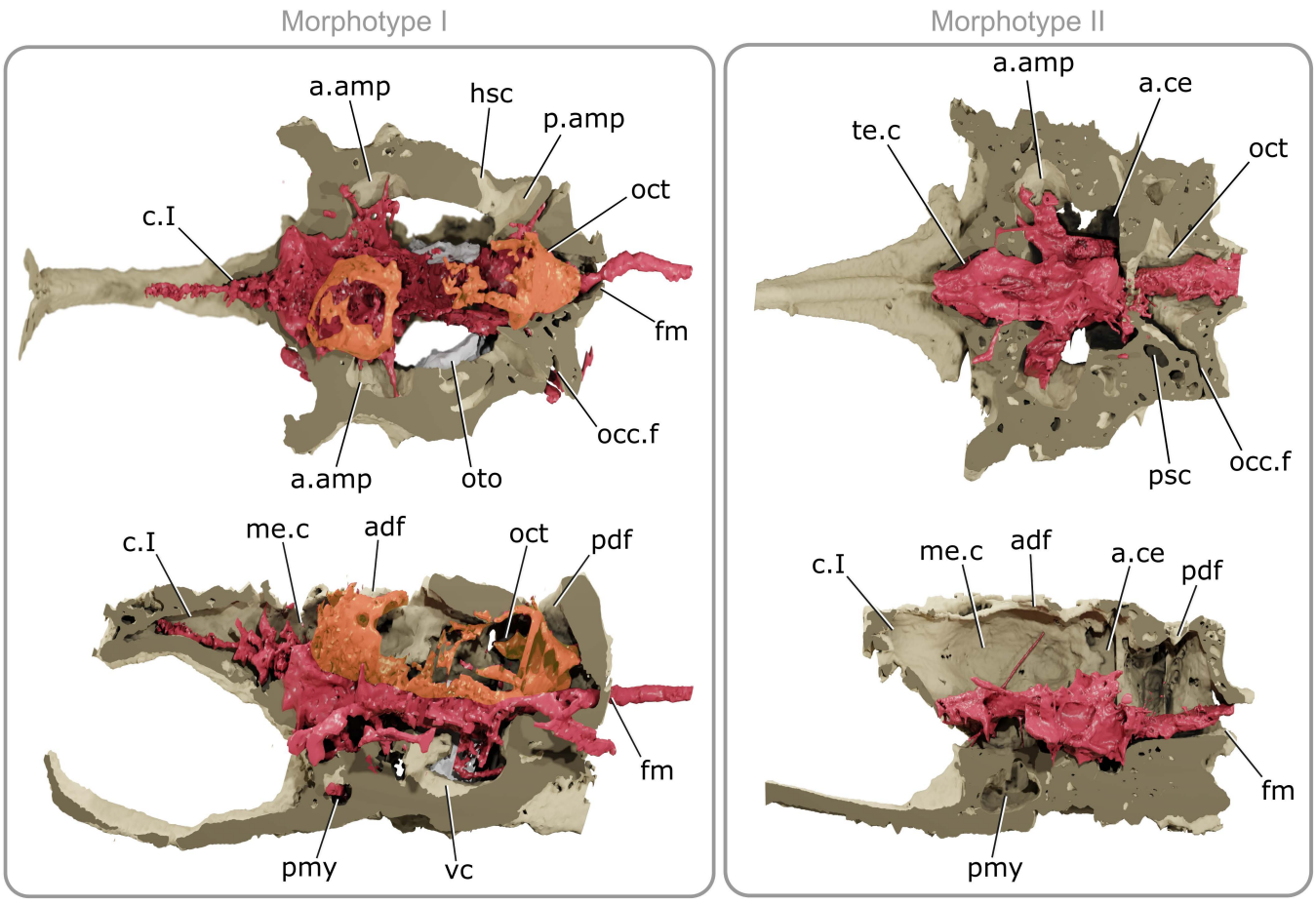
Morphotype I
Morphotype II
a.amp
hsc
p.amp
oct
c.I
fm
occ.f
a.amp
oto
c.I
me.c
adf
oct
pdf
fm
pmy
vc
a.amp
a.ce
te.c
oct
psc
occ.f
c.I
me.c
adf
a.ce
pdf
fm
pmy

Morphotype I

Morphotype II

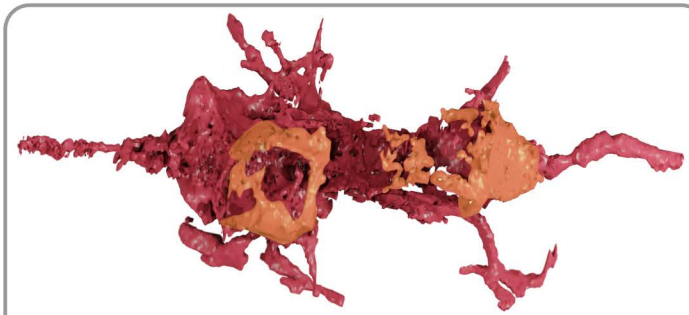

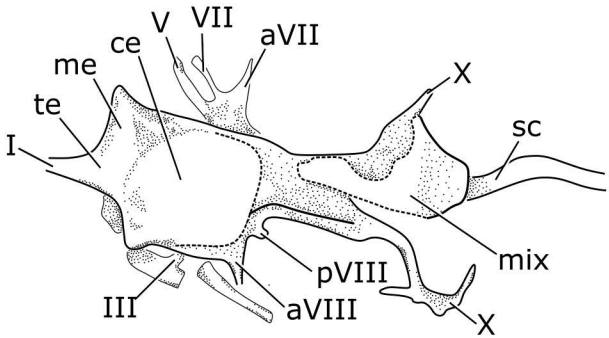

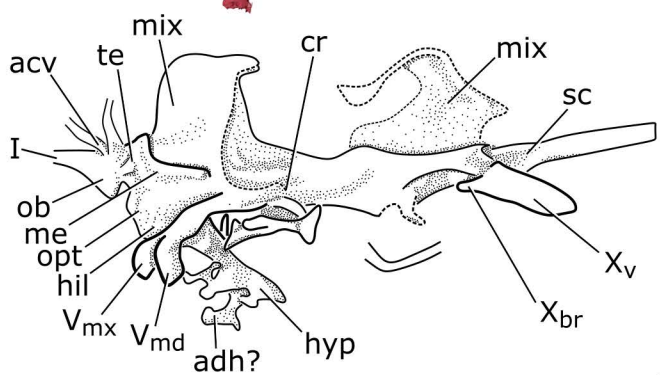

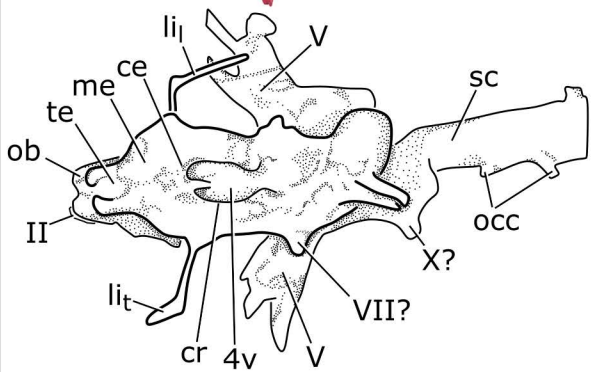

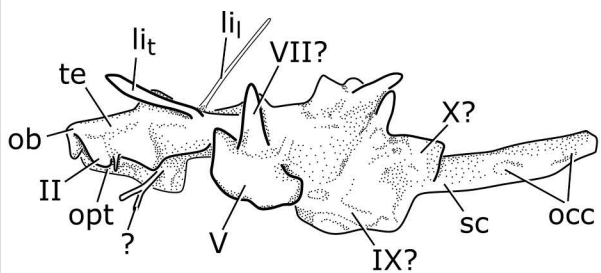

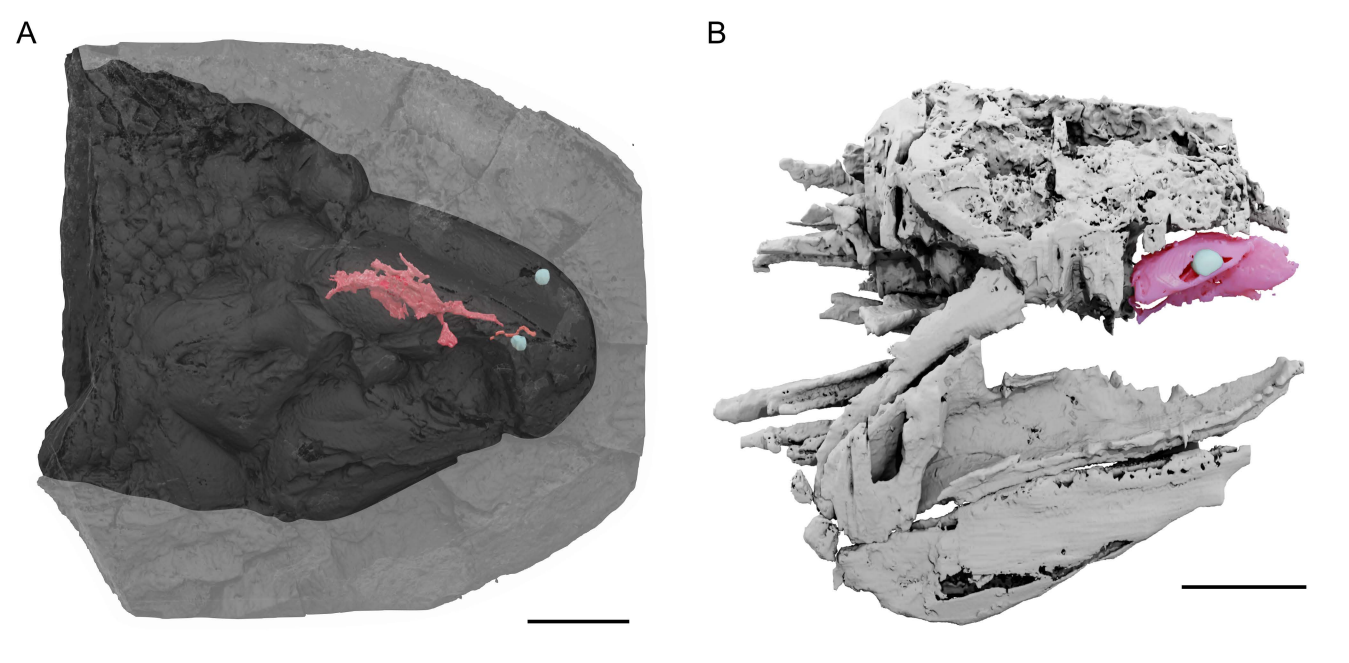
A
B

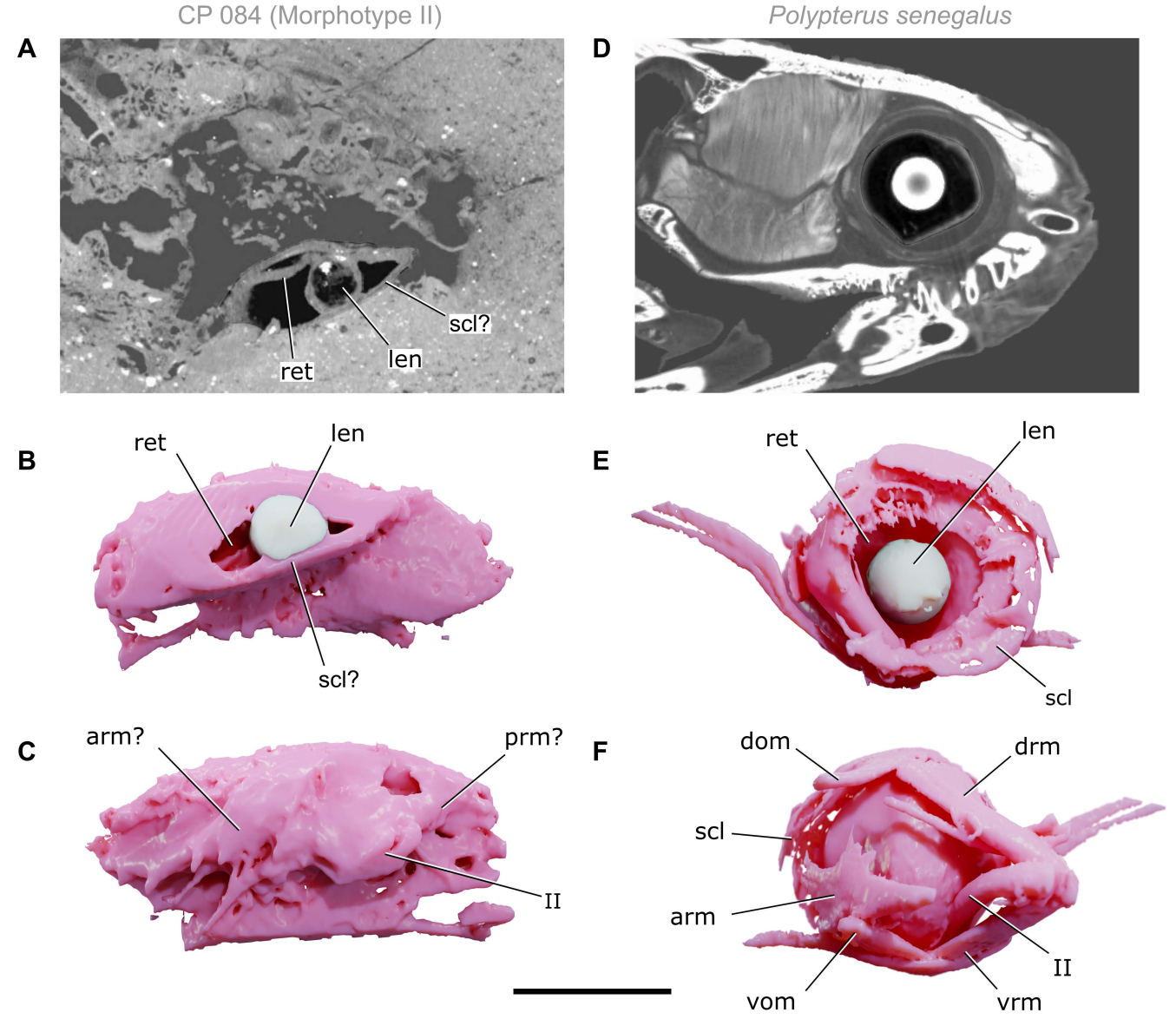
CP 084 (Morphotype II)
Polypterus senegalus
A
ret
len
scl?
D
B
ret
len
scl?
E
ret
len
scl
C
arm?
prm?
II
F
dom
drm
scl
arm
II
vom
vrm

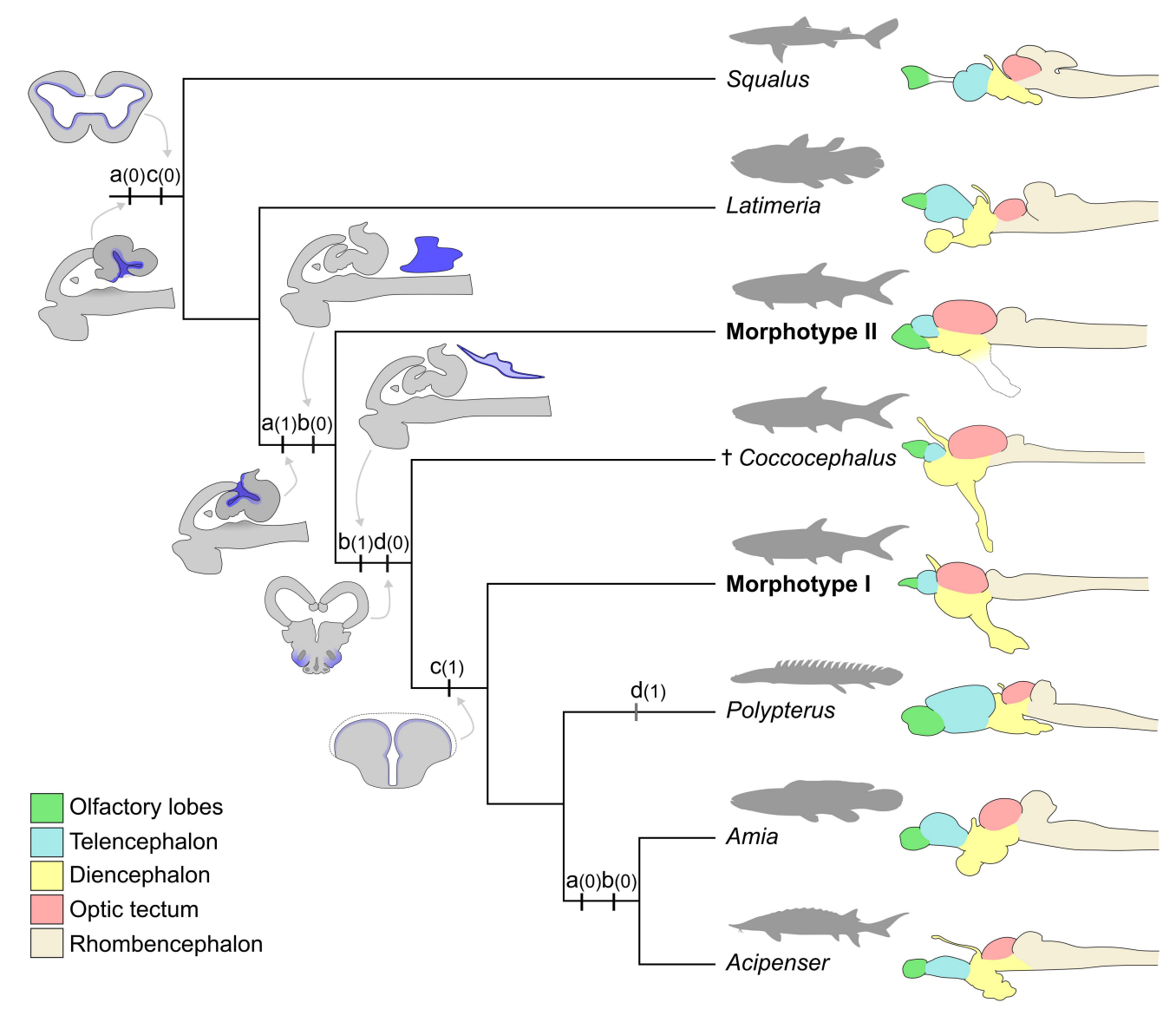
a(0)c(0)
a(1)b(0)
b(1)d(0)
c(1)
d(1)
a(0)b(0)
Squalus
Latimeria
Morphotype II
† Coccocephalus
Morphotype I
Polypterus
Amia
Acipenser
Olfactory lobes
Telencephalon
Diencephalon
Optic tectum
Rhombencephalon

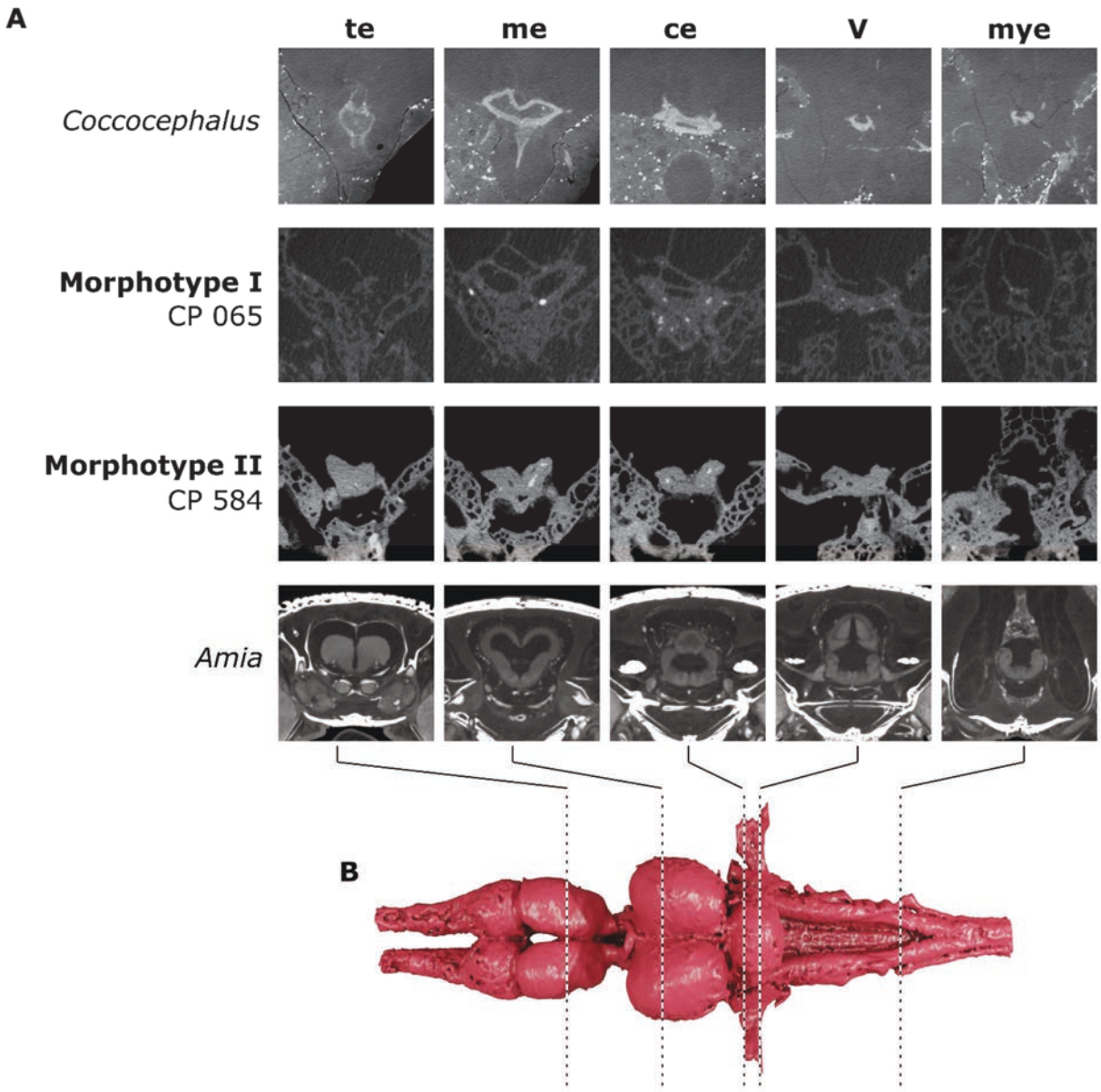

Figure S1. Anatomical correspondence between brains in Paleozoic actinopterygians and *Amia*, Related to Figure 2. (A) axial sections from μCT, beginning with more anterior sections. (B) render of the brain of *Amia* showing approximate position of sections. Abbreviations: tel, telencephalon, mes, mesencephalon, ce, cerebellar corpus, V, trigeminal nerve, mye, myelencephalon.

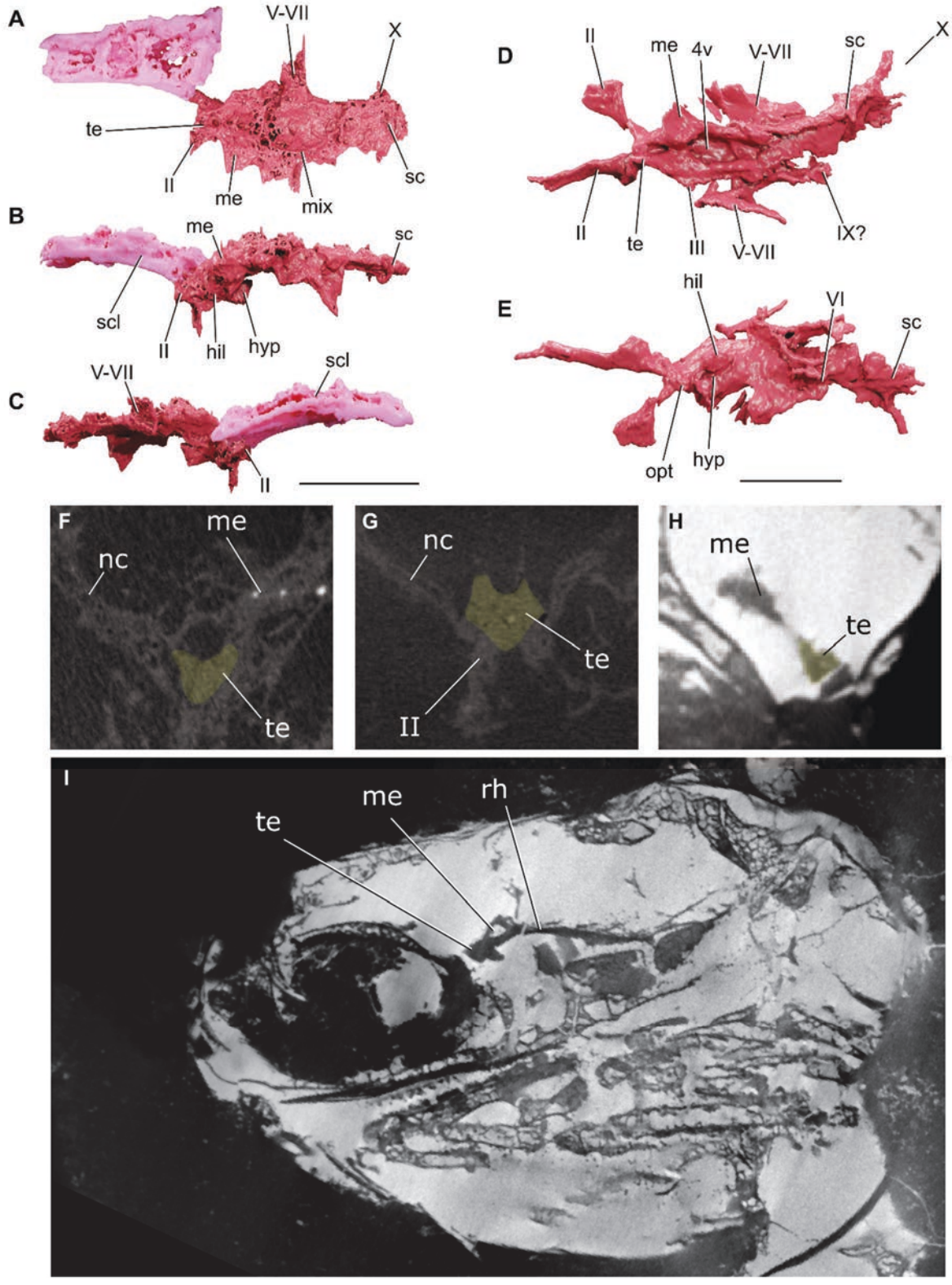
A
V-VII
X
te
II
me
mix
sc
B
me
sc
scl
II
hil
hyp
C
V-VII
scl
II
D
II
me
4v
V-VII
sc
X
II
te
III
V-VII
IX?
E
hil
VI
sc
opt
hyp
F
me
nc
te
G
nc
te
II
H
me
te
I
te
me
rh

Figure S2. Additional brain material, related to Figures 1-3. (A-C) CP.V 4364 (Morphotype I) in (A) dorsal, (B) left-lateral and (C) right-lateral views; and (D-E) CP 508 (Morphotype II) in (D) dorsal and (E) ventral views.(F-I) µCT sections (F) CP 065, (G) CP.V 4364, (H) CP 7053, (I) CP 7053. hil, hypothalamus inferior lobe, hyp, hypophysis, me, mesencephalon, mix, meninx, nc, neurocranium, opt, optic chiasma, rh, rhombencephalon, sc, spinal cord, te, telencephalon, II, optic nerve, III, oculomotor nerve, VI, abducens nerve, V-VII, trigeminofacial nucleus, IX, glossopharyngeal nerve, X, vagus nerve. Scale bars = 5 mm.

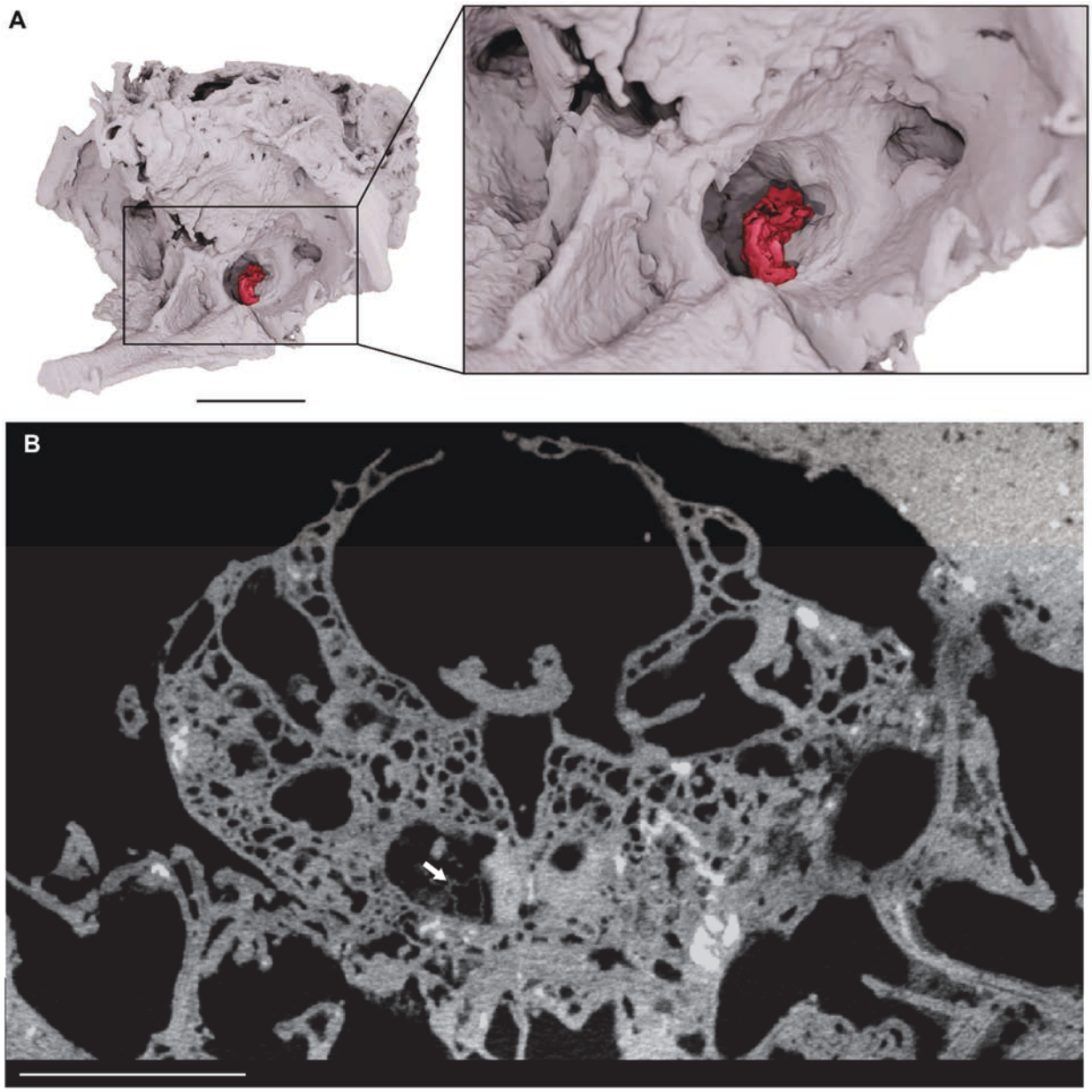

Figure S3. Rectus eye muscle attachment ligament within the posterior myodome of CP 584 (Morphotype II), Related to Figure 5. (A) render of neurocranium (gray) and attachment ligament (red); (B) axial section from µCT showing the attachment ligament (arrow). Scale bar = 5 mm.

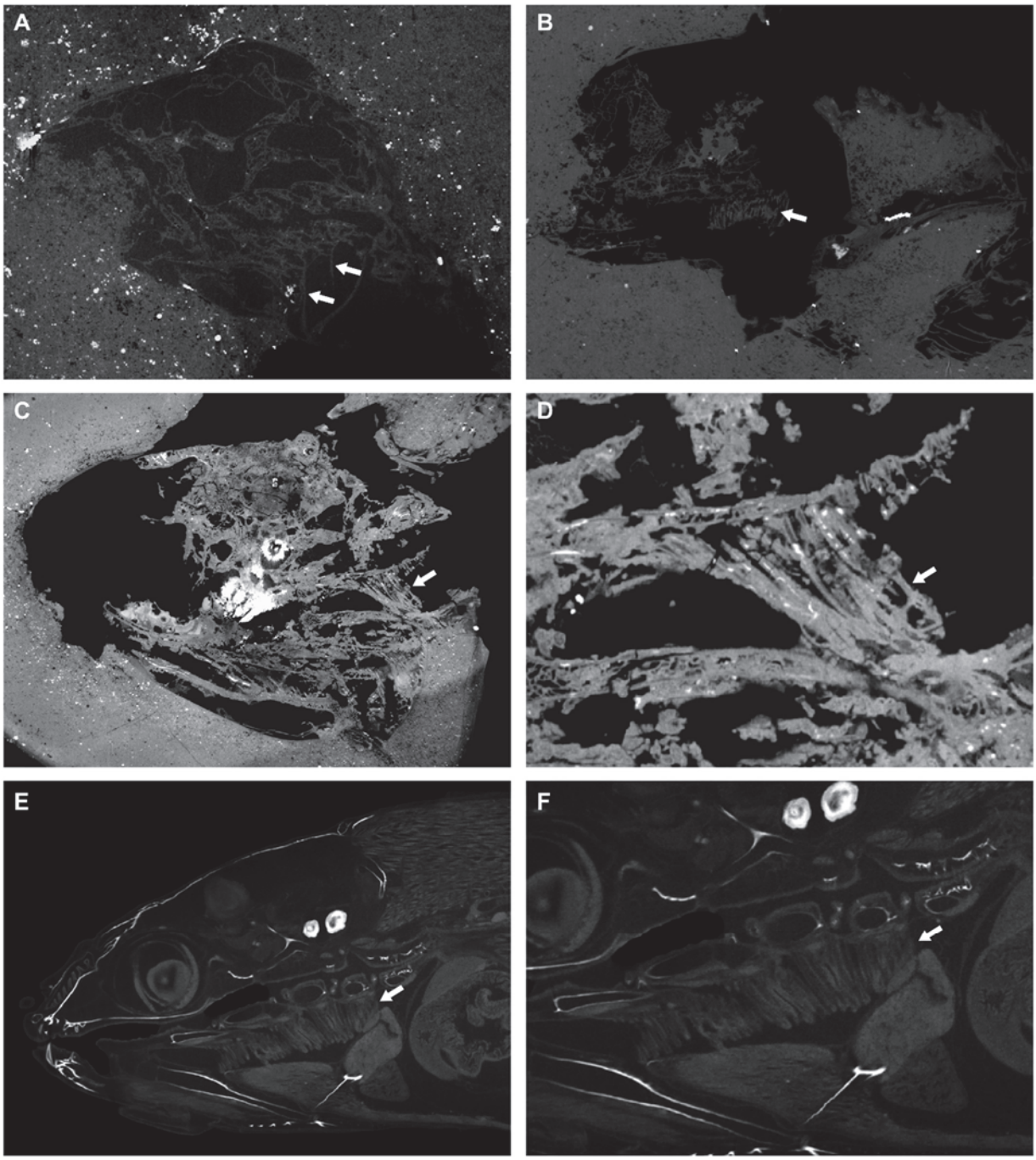

Figure S4. Comparison of gill filaments and lamellae in Permian actinopterygians and *Amia* sp, Related to Figure 4. Based on parasagittal sections derived from µCT scans. (A-B) Morphotype I (A, CP 065, B, CP 7053). (C-D) Morphotype II (CP 084). E-F, *Amia* (UMMZ 160805). Arrows indicate gill filaments. Not to scale.

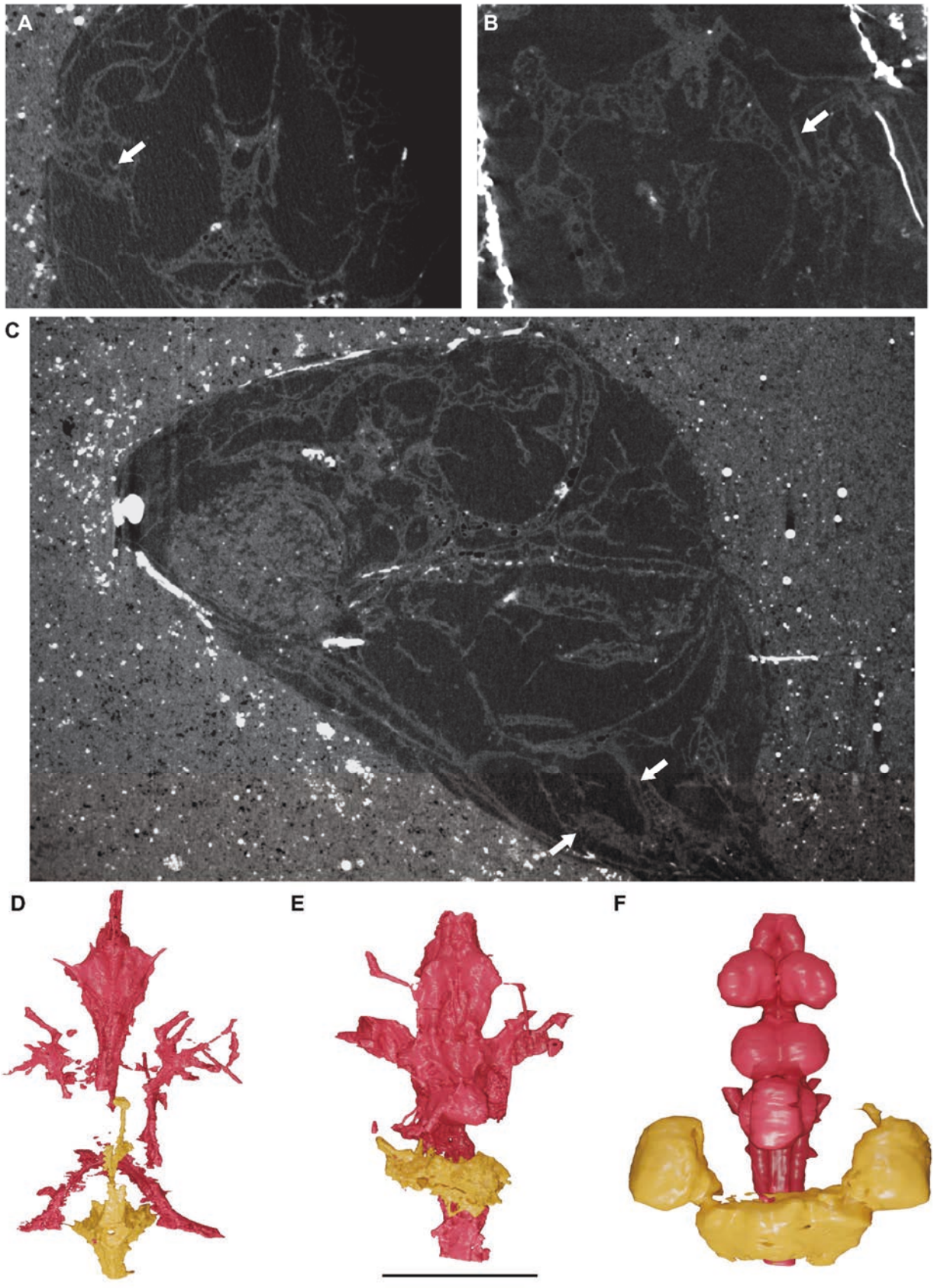
A
B
C
D
E
F

Figure S5. Cardiovascular elements preserved in Permian actinopterygians (Morphotype I), Related to Figure 2. (A) Transverse cross-section through the neurocranium of CP 065 showing the jugal vein (arrow); (B) Horizontal section through the neurocranium of CP 4364 showing the jugal vein (arrow); (C) Sagittal section through the skull of CP 065 showing putative heart tissue preservation (arrows). (D-F) Renders of brains (red) and myelencephalic tissue (orange) in dorsal view. (D) †*Coccocephalus*, (E) CP 584 (Morphotype II), (F) *Lepisosteus oculatus* (UMMZ 196974). (A-C) not to scale, Scale bar = 5 mm (D-E) and 10 mm (F).

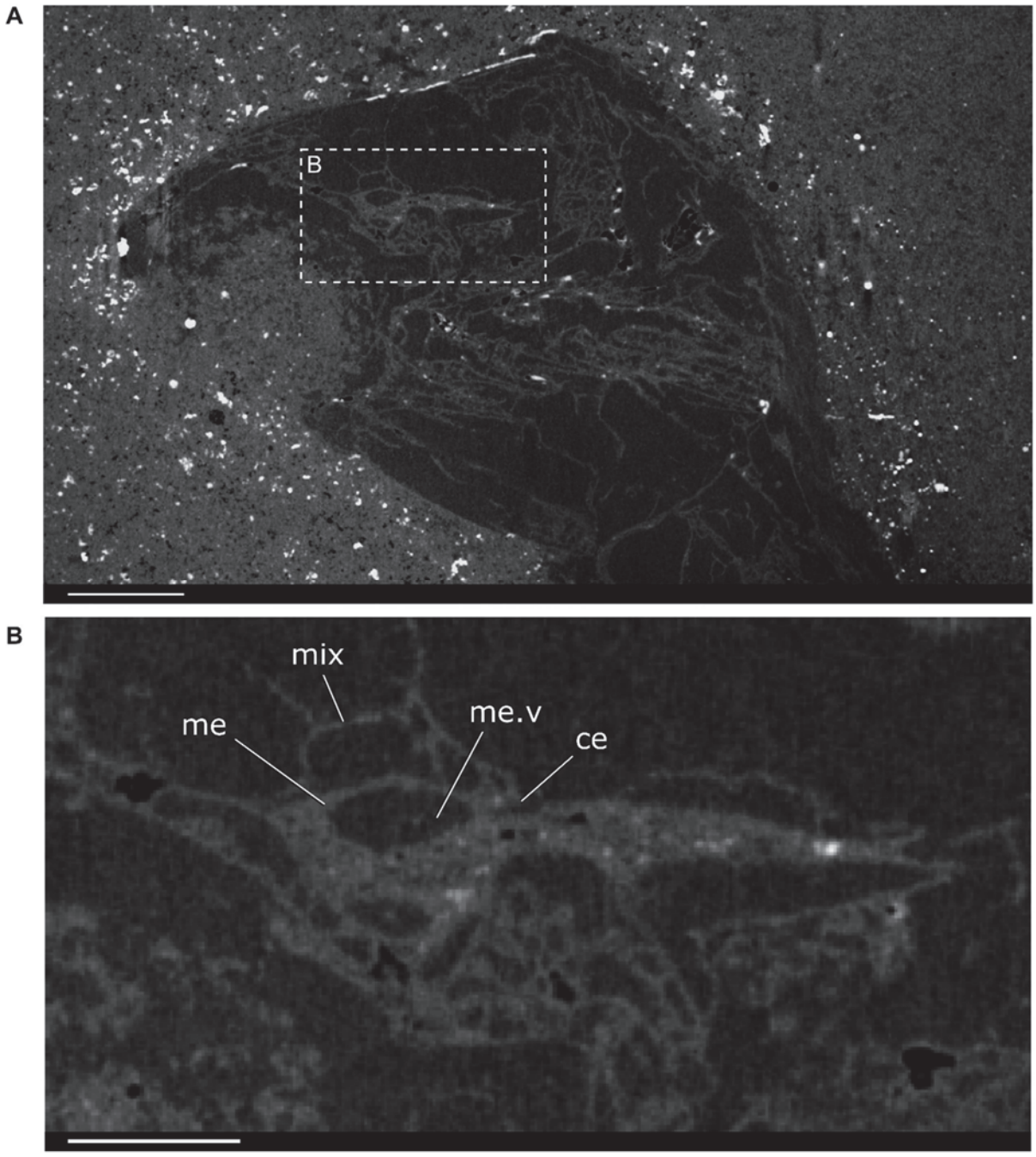

Figure S6. Parasagittal µCT sections through the head of Morphotype I, Related to Figure 1. (A) highlighting the brain (B). ce, cerebellum, exm, extrameningeal space, me, mesencephalon, me.v, mesencephalic ventricle, mix, meningeal tissue. Scale bar = 5 mm (A); Scale bar = 2 mm (B).

	Energy (kV)	Current (uA)	Exposure (s)	Resolution (mm)	Filter	Filter (mm)	Binning	Projections	Frames/Proj.	Ring art.
CP 065	190	180	4	0.03437	Cu	3	NO	3141	4	YES
CP 584	200	180	4	0.03674	Cu	3	NO	3141	2	YES
CP 084	191	200	2	0.04509	Cu	2	NO	3141	4	YES
CP 508	200	180	4	0.03674	Cu	3	NO	3141	2	YES
CP 577	215	148	2.8	0.02638	Cu	2.5	NO	3141	4	YES
CP.V 4364	200	140	2.8	0.02966	Cu	2	NO	3141	2	YES
CP.V 7053	190	180	4	0.03432	Cu	3	NO	3141	2	YES
CP.V 7227	215	120	2.8	0.02046	Cu	2	NO	3141	4	YES
CP 1343	174	190	4	0.03691	-	-	NO	3141	2	YES
CP 6573	195	120	2.8	0.03295	Cu	2.25	NO	3141	4	YES

Table S1. µCT scan parameters used for fossil actinopterygians from the Lontras Shale, Related to STAR Methods.